

Entanglement Dynamics in Three Qubit X -States

Yaakov S. Weinstein¹

¹*Quantum Information Science Group, MITRE, 260 Industrial Way West, Eatontown, NJ 07224, USA*

I explore the entanglement dynamics of a three qubit system in an initial X -state undergoing decoherence including the possible exhibition of entanglement sudden death (ESD). To quantify entanglement I utilize negativity measures and make use of appropriate entanglement witnesses. The negativity results are then extended to X -states with an arbitrary number of qubits. I also demonstrate non-standard behavior of the tri-partite negativity entanglement metric, its sudden appearance after some amount of decoherence followed quickly by its disappearance. Finally, I solve for a lower bound on the three qubit X -state concurrence, demonstrate when this bound goes to zero, and outline simplifications for the calculation of higher order X -state concurrences.

PACS numbers: 03.67.Mn, 03.67.Bg, 03.67.Pp

I. INTRODUCTION

Entanglement is a quantum mechanical phenomenon in which quantum systems exhibit correlations above and beyond what is classically possible. As such it is a crucial resource for many aspects of quantum information processing including quantum computation, quantum cryptography and communications, and quantum metrology [1]. Due to its fundamental, and increasingly practical, importance there is a growing body of literature dedicated to studies of entanglement. Nevertheless, many aspects of entanglement, especially multi-partite entanglement and its evolution, are in need of further exploration [2].

The unavoidable degradation of entanglement due to decoherence has severely hampered experimental attempts to realize quantum information protocols. Decoherence is a result of unwanted interactions between the system of interest and its environment. Highly entangled, and thus highly non-classical, states may be severely corrupted by decoherence [3]. This is especially troubling as these states tend to be the most potentially useful for quantum information protocols. An extreme manifestation of the detrimental effects of decoherence on entanglement is entanglement sudden death (ESD): in which decoherence causes a complete loss of entanglement in a finite time [4, 5] despite the fact that the system coherence goes to zero only asymptotically. Much has been written about this aspect of entanglement for bi-partite systems and there have been several initial experimental studies of this phenomenon [6]. Fewer studies look at ESD, and specifically ESD with respect to multi-partite entanglement, in multi-partite systems [7–11].

A class of two qubit states that are generally known to exhibit ESD are the so called X -states [12], so named due to the pattern of non-zero density matrix elements. These states play an important role in a number of physical systems [13], and allow for easy calculation of certain entanglement measures. In this paper, I explore the entanglement dynamics of three qubit X -states in dephasing and depolarizing environments as a function of decoherence strength. Previous studies of three qubit X -

shaped states utilize more restrictive sets of states: GHZ-diagonal states [14] and generalized GHZ-diagonal states [15]. Other papers have examined specific examples of three qubit X -state entanglement including the effects of dephasing on a three-qubit quantum error correction protocol [16].

To quantify entanglement within the three qubit systems I utilize the negativity, N_j , defined as the most negative eigenvalue of the partial transpose of the density matrix [17] with respect to qubit j . This provides three distinct entanglement measures. As a pure tri-partite entanglement metric for mixed states I will use the tri-partite negativity, $N^{(3)}$ which is simply the third root of the product of the negativities with respect to each of three qubits [18], $N^{(3)} \equiv (N_1 N_2 N_3)^{1/3}$. A mixed state with non-zero $N^{(3)}$ is distillable to a GHZ state. It is important to note the existence of bound entanglement which may be present even if all negativity measures in a three qubit system are equal to zero. Thus, when I refer to ESD of a state with respect to given negativity metrics this should not be confused with separability of the state. Nevertheless, besides general interest in the behavior of these entanglement metrics, the disappearance of negativity plays an important role in quantum information protocols in that it indicates that the entanglement of the state is not distillable.

The physical significance of X -states mentioned above demands and efficient means of experimentally determining the presence of entanglement. This can be accomplished via ‘entanglement witnesses.’ Three qubit states can be separated into four broad categories: separable (in all three qubits), biseparable, and there exist two types of locally inequivalent tri-partite entanglement (GHZ and W-type) [19]. Reference [20] provides a similar classification schemes for mixed states each of which includes within it the previous classes. These are separable (S) states, bi-separable (B) states, W states, and GHZ states, which encompasses the complete set of three qubit states.

Entanglement witnesses are used to determine in which class a given state belongs. These observables give a positive or zero expectation value for all states of a given class and negative expectation values for at least one state in a higher (*i.e.* more inclusive) class. I will make use

of specific entanglement witnesses [20] that will identify whether a state is in the GHZ\W class (*i.e.* a state in the GHZ class but not in the W class), in which case the state has experimentally observable GHZ-type tri-partite entanglement. Though the use of entanglement witness cannot guarantee that entanglement is not present, it does give experimental bounds on whether the entanglement can be observed.

The results presented in this paper are (i) the analytical determination of various negativity measures for X -states of an arbitrary number of qubits including how the negativity evolves under decoherence, (ii) the demonstration that negativity disappears in finite time for X -states subject to different types of decoherence and the (analytical and numerical) determination of the decoherence strength when this occurs, (iii) the analytical calculation of the expectation value of X -states undergoing decoherence with respect to appropriate entanglement witnesses, (iv) the demonstration of the sudden appearance, only at non-zero decoherence strength, in some X -states of the tri-partite negativity, and (v) the calculation of a bound on the three qubit concurrence for X -states and the description of how this can be extended to more qubits. In addition, I prove in the Appendix that the set of generalized GHZ-diagonal states do not cover all possible X -states.

II. THREE QUBIT X -STATES

There are a number of classes of three qubit states whose entanglement properties have been studied and whose non-zero density matrix elements form an X shape:

$$\rho_X(a_j, b_j, c_j) = \begin{pmatrix} a_1 & 0 & 0 & 0 & 0 & 0 & 0 & c_1 \\ 0 & a_2 & 0 & 0 & 0 & 0 & c_2 & 0 \\ 0 & 0 & a_3 & 0 & 0 & c_3 & 0 & 0 \\ 0 & 0 & 0 & a_4 & c_4 & 0 & 0 & 0 \\ 0 & 0 & 0 & c_4^* & b_4 & 0 & 0 & 0 \\ 0 & 0 & c_3^* & 0 & 0 & b_3 & 0 & 0 \\ 0 & c_2^* & 0 & 0 & 0 & 0 & b_2 & 0 \\ c_1^* & 0 & 0 & 0 & 0 & 0 & 0 & b_1 \end{pmatrix} \quad (1)$$

where $j = 1, \dots, 4$. The most basic is a pure three qubit GHZ state with wavefunction $|\psi_k^\pm\rangle = \frac{1}{\sqrt{2}}(|k\rangle \pm |\bar{k}\rangle)$, where k is a three bit binary number between zero and seven and \bar{k} is the result of flipping each bit of k . The density matrix of this state is $\rho_X(1/2_j, 1/2_j, \pm 1/2_j)$. Mixed states that are diagonal in the basis of these eight states form the set of GHZ-diagonal states studied in [14]. The basis states have coefficients $\sqrt{\lambda_k^\pm}$ for all $0 < k < 3$, the squares of which sum to one. The density matrix elements of these states are thus $a_j = b_j = \lambda_k^+ + \lambda_k^-$ and $c_j = \lambda_k^+ - \lambda_k^-$.

A generalized GHZ state is a non-maximally entangled state of the form:

$$|\psi_k^\pm(\alpha, \beta)\rangle = \alpha|k\rangle \pm \beta|\bar{k}\rangle. \quad (2)$$

The density matrix of this state is $\rho_X(|\alpha|_j^2, |\beta|_j^2, \pm\alpha\beta_j^*)$ for $j = 1, \dots, 4$. An incoherent mixture of generalized GHZ states where k now ranges from 0 to 7 (as opposed to 0 to 3 used in in [14]) form a generalized GHZ-diagonal state. These states are studied in [15] and have the form:

$$\rho = \sum_{k=0}^7 \lambda_k^+ |\psi_k^+(\alpha, \beta)\rangle \langle \psi_k^+(\alpha, \beta)| + \lambda_k^- |\psi_k^-(\alpha, \beta)\rangle \langle \psi_k^-(\alpha, \beta)|. \quad (3)$$

For these states the density matrix elements are as follows:

$$a_j = |\alpha|^2(\lambda_k^+ + \lambda_k^-) + |\beta|^2(\lambda_k^+ + \lambda_k^-) \quad (4)$$

$$b_j = |\beta|^2(\lambda_k^+ + \lambda_k^-) + |\alpha|^2(\lambda_k^+ + \lambda_k^-) \quad (5)$$

$$c_j = \alpha\beta^*(\lambda_k^+ - \lambda_k^-) + \alpha^*\beta(\lambda_k^+ - \lambda_k^-) \quad (6)$$

for $1 < j < N/2$ and $k = j - 1$. However, as shown in the Appendix, generalized GHZ-diagonal states do not include all possible X -states. This is due to the restriction of constant α and β for all contributing generalized GHZ states.

In this paper I consider X -states that are completely general, limited only by the restriction that the state is a proper density matrix. For convenience, I will refer to the four density matrix elements a_j, b_j, c_j and c_j^* of the X -state as a GHZ-type state. At most, four GHZ-type states contribute to each three qubit X -state.

III. X -STATE ENTANGLEMENT

An X -state is a mixed state that can be written as a sum of GHZ-type states. When a partial trace is taken over any one of the three qubits of an X -state the resulting two qubit matrix is diagonal. This demonstrates that the entanglement of an X -state is either tri-partite or biseparable but not completely separable. Before calculating any specific entanglement metric and studying its decay in a given decohering environment, we note that an upper bound on the entanglement decay was derived in [15] for a number of different decohering environments. Though these bounds were calculated for the more limited generalized GHZ-diagonal states they appear to be appropriate to the states studied in this work. However, these upper bounds go to zero only in the limit of complete decoherence. Thus, the states never exhibit entanglement sudden death for any entanglement metric and the bounds cannot be used to study the ESD phenomenon. Below, I explore specific entanglement metrics for which I provide analytical solutions to exactly calculate the decoherence strength at which the X -states exhibit ESD for the given entanglement metrics. While ESD of these metrics cannot guarantee separability of the X -state it does provide important information concerning distillability and the ability to determine the presence of entanglement.

To calculate the negativity of a three qubit X -state we take the eigenvalues of the partial transpose of the

density matrix with respect to one of the qubits. These 24 eigenvalues (8 for each possible partial transpose) are all of the form:

$$E_{ij} = \frac{1}{2} \left(a_j + b_j \pm \sqrt{(a_j - b_j)^2 + 4|c_i|^2} \right) \quad (7)$$

for all $i, j = 1, \dots, 4$ and $i \neq j$. From these eigenvalues one can see how the negativity detects the entanglement of an X -state. Let us first assume a GHZ-type state with the only non-zero elements a_j, b_j, c_j and c_j^* . The eigenvalues which utilize elements a_j and b_j cannot be negative (since $a_j + b_j = 1$ and $c_i = 0$ for all $i \neq j$). An additional three eigenvalues will be equal to $-|c_j|$, demonstrating the entanglement in the system. X -states that are sums of two GHZ type states have non-zero elements $a_i, a_j, b_i, b_j, c_i, c_j, c_i^*, c_j^*$. Such states will again have negative eigenvalues $-|c_i|, -|c_j|$ and two additional possibly negative eigenvalues $\frac{1}{2}(a_k + b_k - \sqrt{(a_k - b_k)^2 + 4|c_\ell|^2})$ where $k, \ell = i, j$ and $k \neq \ell$. As more density matrix elements of the X -state are filled up the eigenvalues tend to have the form of these latter two eigenvalues.

A. Dephasing Environment

We now look at the entanglement evolution of the three qubit X -states with no interaction between the qubits, in an independent qubit dephasing environment noting the exhibition of ESD with respect to the negativity. The independent qubit dephasing environment is fully described by the Kraus operators

$$K_1 = \begin{pmatrix} 1 & 0 \\ 0 & \sqrt{1-p} \end{pmatrix}; \quad K_2 = \begin{pmatrix} 0 & 0 \\ 0 & \sqrt{p} \end{pmatrix}, \quad (8)$$

where the dephasing parameter p can also be written in a time-dependent fashion, $p = 1 - \exp(-\kappa t)$. When all three qubits undergo dephasing we have eight Kraus operators each of the form $A_l = (K_i \otimes K_j \otimes K_k)$ where $l = 1, 2, \dots, 8$ and $i, j, k = 1, 2$.

The effect of a dephasing environment of strength p on an X -state is to reduce the anti-diagonal elements of the density matrix by a factor $(1-p)^{3/2}$ while leaving the diagonal elements constant. To calculate the negativity we look at the eigenvalues of the X -state after taking the partial transpose with respect to the desired subsystem. The relevant eigenvalues are now of the form:

$$\frac{1}{2} \left(a_j + b_j - \sqrt{(a_j - b_j)^2 + 4|c_i|^2(1-p)^3} \right). \quad (9)$$

The eigenvalues go to zero when:

$$p = 1 - \frac{(a_j b_j)^{1/3}}{|c_i|^{2/3}}. \quad (10)$$

Based on the above, it is easy to see that ESD with respect to negativity is not exhibited by X -states made

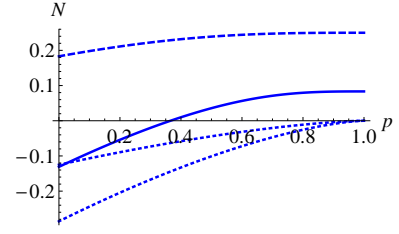


FIG. 1: (Color online) Eigenvalues of partially transposed X -state density matrix with non-zero elements $a_1 = \frac{5}{12}, a_2 = \frac{3}{12}, b_1 = \frac{1}{4}, b_2 = \frac{1}{12}, c_1 = \frac{2}{7},$ and $c_2 = \frac{1}{8}$. When taking the partial transpose with respect to the third qubit there are two ‘negative’ eigenvalues which can be calculated from Eq. 9: $\frac{1}{6} - \frac{1}{84}\sqrt{625 - 576p(3+p(p-3))}$ and $\frac{1}{24}(8 - \sqrt{13 - 9p(3+p(p-3))})$. Using Eq. 10 we can see that only the first of these eigenvalues can be negative and this for $p < .366$. Thus, the state exhibits ESD with respect to N_3 . These two eigenvalues are shown in the plot (solid and dashed line respectively). In addition, the two negative eigenvalues that constitute N_1 and N_2 are shown (dotted lines) neither of these go to zero in finite time. Thus, the state exhibits ESD with respect to the tri-partite negativity at the same value as exhibited for N_3 .

up of single GHZ-type states (with non-zero elements $a_j + b_j = 1$, and c_j): the negativity with respect to any one qubit, and thus the tri-partite negativity as well, is simply $-|c_j|(1-p)^{3/2}$. When the X -state is a mixture of GHZ type states ESD may be exhibited. Fig. 1 shows a sample X -state that is the sum of two GHZ-type states that exhibits ESD with respect to the negativity of the third qubit, N_3 . However, the state does not exhibit ESD with respect to N_1 and N_2 , they are negative for any value of p . The state thus exhibits ESD with respect to the tri-partite negativity at the same dephasing strength as N_3 . For stronger dephasing no tri-partite entanglement is detected.

The above can be compared to the experimental detection capabilities of entanglement witnesses. Appropriate entanglement witnesses for X -states are of the sort:

$$W_k = \frac{3}{4}\mathbb{1} - |GHZ(k)\rangle\langle GHZ(k)| \quad (11)$$

where $|GHZ(k)\rangle = \frac{1}{\sqrt{2}}(|k\rangle + |\bar{k}\rangle)$. For an X -state consisting of a single GHZ-type state the entanglement witness W_k gives $\text{Tr}[W_k \rho] = \frac{1}{4}(1 - 4(1-p)^{3/2}|c_k|)$. Thus, W_k loses its ability to detect entanglement at dephasing strength $p = 1 - \frac{1}{2^{4/3}|c_k|^{2/3}}$. The maximum occurs for $|c_k| = 1/2$ in which case the entanglement is no longer detected at $p = 1 - \frac{1}{2^{1/3}}$. For general X -states the entanglement witnesses give the following:

$$\begin{aligned} \text{Tr}[W_\ell \rho] &= \frac{1}{4}(3(a_i + b_i + a_j + b_j + a_k + b_k) \\ &\quad + a_\ell + b_\ell - 4(1-p)^{3/2}|c_\ell|). \end{aligned} \quad (12)$$

This can be solved for the exact value of p at which the

entanglement is no longer detected:

$$p = 1 - \frac{(3(a_i + b_i + a_j + b_j + a_k + b_k) + a_\ell + b_\ell)^{2/3}}{2^{4/3}|c_\ell|^{2/3}}. \quad (13)$$

I note that which of the above witnesses is most sensitive may depend on the initial state and the decoherence strength and can be determined via a minimization process. What is important is that the witnesses detect purely tri-partite entanglement that does not include biseparable but not completely separable entanglement.

B. Depolarizing Environment

I now look at an independent qubit depolarizing environment and, as above, explore the entanglement evolution of the three qubit X -states. The Kraus operators for this environment are:

$$K_1 = \sqrt{1 - \frac{3p}{4}} \mathbb{1}, K_w = \frac{\sqrt{p}}{2} \sigma_w, \quad (14)$$

where σ_w are the Pauli spin operators, $w = x, y, z$ and p is now the depolarizing strength. The depolarizing environment affects both the anti-diagonal and diagonal elements of the density matrix. The anti-diagonal elements are simply reduced by a factor of $(1 - p)^3$. The diagonal element a_i becomes:

$$\begin{aligned} a'_i &= a_i \left(1 - \frac{3p}{2} + \frac{3p^2}{4} - \frac{p^3}{8}\right) \\ &+ (a_j + a_k + b_\ell) \left(\frac{p}{2} - \frac{p^2}{2} + \frac{p^3}{8}\right) \\ &+ b_i \frac{p^3}{8} + (a_\ell + b_j + b_k) \left(\frac{p^2}{4} - \frac{p^3}{8}\right) \end{aligned} \quad (15)$$

where if $(i, \ell) = (1, 4)$, $(j, k) = (2, 3)$ and vice versa. For the b'_i elements simply replace each term b_l with a_l and each a_l with b_l , for $l = 1, \dots, 4$. Since the decohering environment preserves the X shape of the density matrix the eigenvalues of the partially transposed density matrix follow Eq. 7 and the critical value of p for which a given eigenvalue goes from negative to positive can be analytically determined.

When the initial density matrix is composed of only one GHZ-type state eigenvalues of the partially transposed density matrix are the same for each qubit and the state exhibits ESD at the same depolarizing strength for all N_j and $N^{(3)}$. When the X -state density matrix is a mixture of multiple GHZ-type states ESD may be exhibited with respect to specific negativity measures at different depolarizing strengths. Figure 2 shows the lowest eigenvalue of the partially transposed density matrix with respect to each of the three qubits for a sample X -state composed of a mixture of GHZ-type states as a function of decoherence strength. One eigenvalue is always positive (*i.e.* indicating zero negativity) and two of the eigenvalues cross zero (*i.e.* the state undergoes ESD

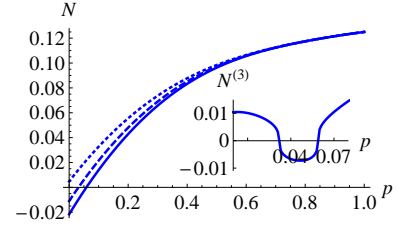


FIG. 2: (Color online) Eigenvalues of partially transposed X -state density matrix with non-zero elements $a_1 = \frac{1}{8}, a_2 = \frac{1}{8}, a_3 = \frac{1}{8}, a_4 = \frac{1}{16}, b_1 = \frac{1}{8}, b_2 = \frac{1}{8}, b_3 = \frac{3}{16}, b_4 = \frac{1}{8}, c_1 = \frac{1}{12}, c_2 = \frac{1}{9}, c_3 = \frac{1}{10}$, and $c_4 = \frac{2}{25}$. The most negative eigenvalue is shown for the partial transpose of the initial X -state density matrix taken with respect to the first (dotted line), second (solid line), and third (dashed line) qubit. The state exhibits ESD with respect to the latter two negativities at dephasing values $p \simeq .0585$ and $.0317$, respectively. The inset shows the tri-partite negativity. Note that this tri-partite entanglement measure goes from positive (indicating the lack of $N^{(3)}$ entanglement) to negative (indicating the presence of GHZ distillable entanglement), back to positive. This entanglement behavior arises from the fact that the single qubit negativities cross zero at different decoherence strengths.

with respect to the single qubit negativities) at different decoherence strengths. For low values of p two of the lowest eigenvalues are negative demonstrating the presence of entanglement. However, there is no measurable GHZ distillable tri-partite entanglement as measured by $N^{(3)}$. For slightly higher values of p there is a small region for which only one of the eigenvalues is negative. Now $N^{(3)}$ becomes negative showing a sudden *birth* of (GHZ distillable) tri-partite negativity. As p increases further, the state exhibits ESD with respect to all single qubit negativities and $N^{(3)}$ (and N_2) becomes positive. This sort of $N^{(3)}$ behavior indicates that there is only a small region of decoherence strengths (which does not include $p = 0$) for which we can be sure there exists GHZ-distillable entanglement. Such behavior, going from positive to negative and back, cannot occur when the X -state is composed of only two GHZ-type states. This is because two of the single qubit negativities are equal, the partial trace with respect to two of the qubits give the same set of eigenvalues. The sign of $N^{(3)}$ is thus determined solely by the eigenvalues of the partially transposed state with respect to the third qubit. An example of a state exhibiting the sudden birth of $N^{(3)}$ entanglement followed by an exhibition of ESD is portrayed in the inset of Fig. 2.

To test for the presence of purely tri-partite entanglement in the depolarizing system we look at the expectation value of the state with an entanglement witness. Using the witnesses defined above we note that witness W_j for a state depolarized with a strength p gives:

$$\begin{aligned} \text{Tr}[W_j \rho] &= \frac{1}{8}(p^2 - 2p + 6) \left(\sum_{i \neq j} a_i + b_i \right) \\ &- \frac{1}{8}(3p^2 - 6p - 2)(a_j + b_j) + (p - 1)^3 c_j \end{aligned} \quad (16)$$

This equation can then be solved for the critical decoherence strength at which entanglement will no longer be detected.

IV. X-STATES WITH MORE QUBITS

The particular matrix structure of the X -state allows us to extend our results beyond three qubits. A matrix with non-zero elements in an X shape can be block diagonalized with blocks of size 2×2 . Assuming the X -matrix elements along the diagonal are d_1, \dots, d_N , and the elements along the anti-diagonal are e_1, \dots, e_N (starting at the top right), the m th 2×2 block along the diagonal has elements:

$$A_m = \begin{pmatrix} d_m & e_m \\ e_{N-m+1} & d_{N-m+1} \end{pmatrix}; \quad (17)$$

where $1 \leq m \leq N/2$. Thus, the eigenvalues of any dimension X -shaped matrices are simply the eigenvalues of the 2×2 blocks which are

$$\frac{1}{2}(d_m + d_{N-m+1} \pm \sqrt{(d_m - d_{N-m+1})^2 + 4e_m e_{N-m+1}}). \quad (18)$$

When calculating the negativity a partial transpose of the density matrix must be taken. This has the effect of rearranging only the elements along the anti-diagonal while preserving the X shape. Thus, the eigenvalues of the partial transpose of an X -state of any dimension have the form of Eq. 7 and the negativity is easily calculated.

V. THREE-QUBIT CONCURRENCE

In this section I derive an explicit expression for a lower bound of three qubit mixed state concurrence as defined in [21] for X -states. A general expression for a lower bound on the three-qubit concurrence is:

$$\tau_3 = \sqrt{\frac{1}{3} \sum_{\ell=1}^6 [(C_\ell^{12|3})^2 + (C_\ell^{13|2})^2 + (C_\ell^{23|1})^2]}. \quad (19)$$

Each of the three bi-partite concurrence terms $C_\ell^{ij|k}$ is given as the sum of the six terms:

$$C_\ell = \max\{0, \sqrt{\lambda_\ell^1} - \sqrt{\lambda_\ell^2} - \sqrt{\lambda_\ell^3} - \sqrt{\lambda_\ell^4}\}, \quad (20)$$

where λ_ℓ^i are the non-zero eigenvalues of $\tilde{\rho} = \rho S_\ell^{ij|k} \rho^* S_\ell^{ij|k}$ in descending order. The operators $S_\ell^{ij|k}$ are given by $S_\ell^{ij|k} = L_\ell^{ij} \otimes L_0^k$ where L_ℓ^{ij} is one of six generators of the group $SO(4)$ operating on qubits i, j , and L_0^k is the generator of $SO(2)$, the Pauli matrix σ_y , operating on qubit k . This lower bound on mixed state concurrence has been calculated for some simple X -states in [22]. Here I look to extend these results and note where

the lower bound goes to zero. Once the lower bound does go to zero, there is no longer a guarantee that entanglement is present.

For initial density matrices that are X -states only six of the 18 contributing terms to the three qubit concurrence are non-zero. More specifically, only the two $SO(4)$ generators with elements on the anti-diagonal contribute to each of the three bi-partite concurrences. I will refer to the $SO(4)$ generator with anti-diagonal $(-1, 0, 0, 1)$ as L_1^{ij} , and the $SO(4)$ generator with anti-diagonal $(0, -1, 1, 0)$ as L_2^{ij} . For X -states the four eigenvalues that make up each of the six terms are of the form:

$$\lambda_{\ell, m_\pm}^{ij|k} = a_m b_m + |c_m|^2 \pm 2\sqrt{a_m b_m |c_m|^2} \quad (21)$$

for two different values of m . For the partition $12|3$ and $SO(4)$ generator $\ell = 1$ the contributing terms have $m = 1, 2$. For the generator $\ell = 2, m = 3, 4$. Similarly, for the partition $23|1$ we find $\ell = 1, m = 2, 3$ and $\ell = 2, m = 1, 4$. Finally, for the $13|2$ partition $\ell = 1, m = 2, 4$ and $\ell = 2, m = 1, 3$. Given these eigenvalues the three-concurrence can be easily computed.

A. Dephasing Environment

For X -states composed of only one GHZ-type state an exact calculation for τ_3 in a dephasing environment yields the maximum between 0 and:

$$\sqrt{a_i - a_i^2 + c_i(-\omega_i + 2\gamma_i^{\frac{1}{2}})} - \sqrt{a_i - a_i^2 + c_i(-\omega_i - 2\gamma_i^{\frac{1}{2}})} \quad (22)$$

where,

$$\begin{aligned} \omega_i &= c_i(p-1)^3 \\ \gamma_i &= a_i(a_i-1)(p-1)^3. \end{aligned} \quad (23)$$

Eq. 22 goes to zero only in the limit of $p \rightarrow 1$. Thus, the lower bound cannot go to zero for a GHZ-type state, some entanglement will always be present. In fact, the lower bound cannot go to zero unless the X -state is composed of four GHZ-type states. This is because τ_3 is a summation of terms and can go to zero only if each term goes to zero. Each one of these (six) terms consists of four eigenvalues, two for each of two m values. If the eigenvalues of one of the m values are zero (which will happen if c_i and a_i or $b_i = 0$) the term will have the form of Eq. 22. Thus, that term, if not initially zero, will remain non-zero until $p = 1$. This behavior is demonstrated in Fig. 3 and should be contrasted with the negativity and tripartite negativity measures. The negativity of X -states can go to zero in a dephasing channel when the X -state is composed of only two GHZ-type states. The reason for this is that the negativity can be defined with respect to only one of the qubits (for example N_3) which may go to zero while negativity measures with respect to the other qubits do not. The three qubit concurrence, however, is a sum over all terms and therefore cannot go to zero unless each bi-partite concurrence term goes to zero.

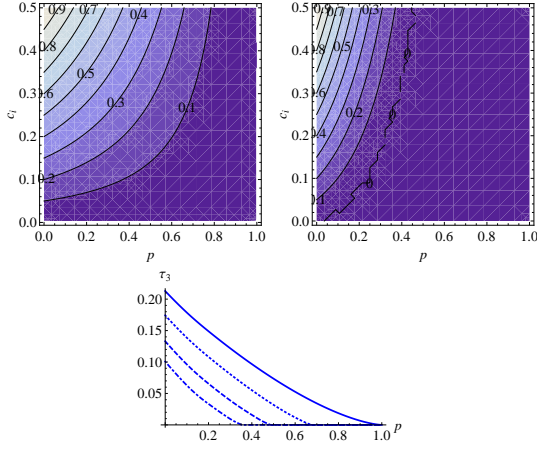


FIG. 3: (Color online) Top row: Three qubit concurrence for X -states composed of one GHZ-type state with $a_i = b_i = 1/2$. Left: in a dephasing environment τ_3 never goes to zero. Right: in a depolarizing environment τ_3 goes to zero when $\frac{1}{4}(p(p-2) + 8c_1(1-p)^3) = 0$. Bottom: example of three-qubit concurrence evolution as a function of dephasing strength. The chosen X -state density matrix is: $a_1 = \frac{3}{8} - \epsilon$, $a_2 = \frac{1}{4}$, $a_3 = \epsilon$, $a_4 = \frac{1}{16}$, $b_1 = \frac{1}{16}$, $b_2 = \frac{1}{16}$, $b_3 = \frac{1}{16}$, $b_4 = \frac{1}{8}$, $c_1 = \frac{3}{25}$, $c_2 = \frac{1}{9}$, $c_3 = \frac{\epsilon}{2}$, and $c_4 = \frac{1}{12}$. τ_3 is shown for $\epsilon = 0$ (solid line), $\epsilon = 1/128$ (dotted line), $\epsilon = 1/32$ (dashed line), and $\epsilon = 1/16$ (chained line). Note that when $a_3 = 0$ τ_3 does not go to zero. Adding any finite amount to a_3 allows τ_3 to go to zero.

B. Depolarizing Environment

The bound on the three-qubit concurrence for X -states composed of one GHZ-type state in a depolarizing environment gives the maximum between 0 and:

$$\frac{q_i}{4} - \sqrt{\omega_i^2 - \frac{\gamma_i'}{64} - \frac{\sqrt{\omega_i^2 \gamma_i'}}{4}} + \sqrt{\omega_i^2 - \frac{\gamma_i'}{64} + \frac{\sqrt{\omega_i^2 \gamma_i'}}{4}} \quad (24)$$

where,

$$q_i = (p-2)p\sqrt{4(p-1)^2(a_i - a_i^2) - p(p-2)} \quad (25)$$

$$\gamma_i' = (a_i(p-2)^3 + (a_i - 1)p^3)((a_i - 1)(p-2)^3 + a_1 p^3).$$

τ_3 for this state is shown in Fig. 3 for an initial state $a_i = b_i = 1/2$. For the depolarizing environment τ_3 can go to zero even for X -states composed of only one GHZ-type state.

The matrix $\tilde{\rho}$ for a X -state density matrix with any of the six $\text{SO}(4)$ generators retains its X shape, having four diagonal and four anti-diagonal elements (and thus have only four non-zero eigenvalues as noted in [21]). The X is ‘balanced’ when $S_\ell^{ij|k}$ is anti-diagonal. I use the term ‘balanced’ as follows: any diagonal X -matrix element d_m that is non-zero has a non-zero counterpart element e_m , where I have used the notation of Eq. 17. An unbalanced X -matrix will have non-zero elements whose counterparts are zero. When a balanced X -matrix is block diagonalized non-zero 2×2 blocks will have four

non-zero elements leading to non-degenerate eigenvalues like those of Eq. 18. Block diagonalized unbalanced X -matrices will have a zero in one of the off-diagonal elements of the 2×2 diagonal block as can be noted from Eq. 17. In the unbalanced case the eigenvalues are then simply the diagonal elements of the block which are of the form $a_i b_j, a_i b_j, a_k b_l, a_k b_l$. These elements (eigenvalues) are degenerate and thus these bi-partite concurrence terms equal zero.

C. n -Qubit Concurrence

As mentioned above, only the two $\text{SO}(4)$ generators with elements on the anti-diagonal, contribute to the three qubit concurrence. This is because only these two generators have anti-diagonal elements which lead to balanced X -matrices $\tilde{\rho}$. The other generators lead to unbalanced $\tilde{\rho}$ matrices whose eigenvalues are simply its diagonal elements. The eigenvalues are each doubly degenerate meaning that these terms will not contribute to the concurrence. The above allows us to simplify calculations for higher qubit concurrences of X -states. The only terms necessary to calculate are those that utilize anti-diagonal $S_\ell^{ij\dots|k\ell\dots}$ matrices. Thus, for four qubits there would be four terms from the $\text{SO}(4) \otimes \text{SO}(4)$ generators for each of the three balanced partitions (two qubits on each side of the partition) and an additional four terms from the $\text{SO}(8) \otimes \text{SO}(2)$ generators for each of the four unbalanced partitions (partitions of three and one qubit). This gives a total of 28 terms which should significantly simplify these calculations.

VI. CONCLUSIONS

In this paper I have studied the entanglement dynamics for three qubit X -states in both dephasing and depolarizing environments. To do this I have analytically calculated the eigenvalues of partial transposes of the X -states which allows for easy determination of the negativity. Since the dephasing and depolarizing environments retain the density matrix X shape one can calculate which initial states will exhibit ESD with respect to the negativity measures and at what decoherence strength. I noted that the tri-partite negativity, a tri-partite entanglement measure which is sufficient to ensure GHZ distillability, can exhibit non-standard behavior for certain X -states: its appearance only at non-zero decoherence strength followed by its sudden disappearance. In addition, I explored the detection capability of entanglement witnesses sensitive to tri-partite entanglement. As with the negativity, the expectation value of the X -state with respect to the entanglement witness can be solved analytically and are vital in assessing potential experimental studies. These results are extended to systems made of arbitrary numbers of qubits. Finally, I analytically solved for the relevant terms of a lower bound on the three-qubit

concurrence for an X -state, demonstrated when it goes to zero in dephasing and depolarizing environments. This method may be useful for calculating concurrences for larger numbers of qubits.

It is a pleasure to thank G. Gilbert and S. Papapas for helpful feedback and acknowledge support from the MITRE Innovation Program under MIP grant #20MSR053.

Appendix A: General X-States

As mentioned in the main part of the paper, a previously studied set of states with an X shaped density matrix is the generalized GHZ-diagonal states [15]. In this Appendix I prove that generalized GHZ-diagonal states do not include all possible X -states by constructing an explicit state with an X -shaped density matrix that is not part of the aforementioned set.

Generalized GHZ-diagonal states with n qubits have the form

$$\rho = \sum_{k=0}^{N-1} \lambda_k^+ |\psi_k^+(\alpha, \beta)\rangle \langle \psi_k^+(\alpha, \beta)| + \lambda_k^- |\psi_k^-(\alpha, \beta)\rangle \langle \psi_k^-(\alpha, \beta)|, \quad (\text{A1})$$

where $N = 2^n$ is the Hilbert space dimension. The density matrix elements of these states using the notation of Eq. 1 are as follows:

$$a_j = |\alpha|^2(\lambda_k^+ + \lambda_k^-) + |\beta|^2(\lambda_k^+ + \lambda_k^-) \quad (\text{A2})$$

$$b_j = |\beta|^2(\lambda_k^+ + \lambda_k^-) + |\alpha|^2(\lambda_k^+ + \lambda_k^-) \quad (\text{A3})$$

$$c_j = \alpha\beta^*(\lambda_k^+ - \lambda_k^-) + \alpha^*\beta(\lambda_k^+ - \lambda_k^-) \quad (\text{A4})$$

for $1 < j < N/2$ and $k = j - 1$.

We now construct an X -state that is not a generalized GHZ-diagonal state. Let us set $c_j = 0$. There are then three possible solutions for Eq. A4:

$\alpha = 0$ or $\beta = 0$

If either of these is true then all other c_m for $m \neq j$ must also equal zero.

$$\lambda_k^+ = \lambda_k^- \text{ and } \lambda_k^+ = \lambda_k^-$$

If this is true $a_j = 2(|\alpha|^2\lambda_k + |\beta|^2\lambda_k^-)$ and $b_j = 2(|\beta|^2\lambda_k + |\alpha|^2\lambda_k^-)$ where $\lambda_k = \lambda_k^+ = \lambda_k^-$. Therefore, if in addition $b_j = 0$ (which would require $\lambda_k = \lambda_k^- = 0$), a_j must equal zero.

$$(\lambda_k^+ - \lambda_k^-) = \frac{\alpha^*\beta}{\alpha\beta^*}(\lambda_k^- - \lambda_k^+)$$

Let $\alpha^*\beta = re^{i\theta}$ where r, θ are real. Then the fraction $\frac{\alpha^*\beta}{\alpha\beta^*} = e^{2i\theta}$. As mentioned in the main part of the paper, the coefficients λ are all real forcing $e^{2i\theta}$ to be real and $\theta = 0, m\pi$ for all integers m . Therefore, $\alpha^*\beta$ and $\alpha\beta^*$ must both be purely real or purely imaginary.

We can now explicitly construct a two qubit X -state that is not part of the set of generalized GHZ-diagonal states by setting $c_1 = 0$ and violating each of the three conditions listed above. Such a state can have the form:

$$\rho_C = \begin{pmatrix} a_1 & 0 & 0 & 0 \\ 0 & a_2 & re^{i\phi} & 0 \\ 0 & re^{-i\phi} & b_2 & 0 \\ 0 & 0 & 0 & 0 \end{pmatrix}. \quad (\text{A5})$$

where r, θ are real and $r^2 < a_2b_2$ guarantees the density matrix has positive eigenvalues. In addition, ρ_C must be trace 1, $a_1 + a_2 + b_2 = 1$, and its purity must be $a_1^2 + a_2^2 + b_2^2 + 2r^2 \leq 1$.

In Eq. A5 $c_1 = 0$, yet $c_2 \neq 0$, indicating that $\alpha, \beta \neq 0$. Furthermore, $b_1 = 0$ while a_1 does not, indicating that $\lambda_0^+ = \lambda_0^-$ and $\lambda_3^+ = \lambda_3^-$ cannot both be true. Finally, $c_2 = re^{i\phi}$ need not be real nor purely imaginary indicating that $(\lambda_0^+ - \lambda_0^-) \neq \frac{\alpha^*\beta}{\alpha\beta^*}(\lambda_3^- - \lambda_3^+)$. Thus, the state ρ_C is not part of the set of generalized GHZ-diagonal states though it certainly is an X -state.

-
- [1] M Nielsen, I. Chuang, *Quantum information and Computation* (Cambridge University Press, Cambridge, 2000).
 - [2] For a recent review see R. Horodecki, P. Horodecki, M. Horodecki, K. Horodecki, Rev. Mod. Phys. **81**, 865 (2009).
 - [3] C. Simon and J. Kempe, Phys. Rev. A **65**, 052327 (2002); W. Dur and H.-J. Briegel, Phys. Rev. Lett. **92** 180403 (2004); M. Hein, W. Dur, and H.-J. Briegel, Phys. Rev. A **71**, 032350 (2005); S. Bandyopadhyay and D.A. Lidar, Phys. Rev. A **72**, 042339 (2005); O. Guhne, F. Bodosky, and M. Blaauuboer, Phys. Rev. A **78**, 060301 (2008).
 - [4] P.J. Dodd and J.J. Halliwell, Phys. Rev. A **69**, 052105 (2004).
 - [5] T. Yu and J.H. Eberly, Phys. Rev. Lett. **93**, 140404 (2004); *ibid.* **97**, 140403 (2006).
 - [6] M.P. Almeida, *et al.*, Science **316**, 579 (2007); J. Laurat, K.S. Choi, H. Deng, C.W. Chou, and H.J. Kimble, Phys. Rev. Lett. **99**, 180504 (2007); A. Salles, F. de Melo, M.P. Almeida, M. Hor-Meyll, S.P. Walborn, P.H. Souto Ribeiro, and L. Davidovich, Phys. Rev. A **78**, 022322 (2008).
 - [7] L. Aolita, R. Chaves, D. Cavalcanti, A. Acin, and L. Davidovich, Phys. Rev. Lett. **100**, 080501 (2008).
 - [8] C.E. Lopez, G. Romero, F. Lastra, E. Solano, and J.C. Retamal, Phys. Rev. Lett. **101**, 080503 (2008).
 - [9] M. Yonac, T. Yu, J.H. Eberly, J. Phys. B **39**, 5621 (2006); *ibid.* **40**, 545 (2007).
 - [10] Y.-K. Bai, M.-Y. Ye, Z.D. Wang, Phys. Rev. A **80**, 044301 (2009).
 - [11] Y.S. Weinstein, Phys. Rev. A **79**, 052325 (2009); *ibid.* **80**, 022310 (2009).
 - [12] T. Yu and J.H. Eberly, Quant. Inf. Comp. **7**, 459, (2007); M.Ali, G. Alber, and A.R.P. Rau, J. Phys. B **42**, 025501 (2009); A.R.P. Rau, J. Phys. A **42**, 412002 (2009).

- [13] For example the model of J. Li, G.S. Paraoanu, Eur. Phys. J. D **56**, 255 (2010).
- [14] O. Guhne and M. Seevinck, New J. Phys. **12**, 053002 (2010).
- [15] L. Aolita, D. Cavalcanti, A. Acin, A. Salles, M. Tiersch, A. Buchleitner, and F. de Melo, Phys. Rev. A **79**, 032322 (2009).
- [16] Y.S. Weinstein, Phys. Rev. A **79**, 012318 (2009).
- [17] G. Vidal and R.F. Werner, Phys. Rev. A **65**, 032314 (2002).
- [18] C. Sabin and G. Garcia-Alcaine, Eur. Phys. J. D **48**, 435 (2008).
- [19] W. Dur, G. Vidal, and J.I. Cirac, Phys. Rev. A **62**, 062314 (2000).
- [20] A. Acin, D. Bruß, M. Lewenstein, A. Sanpera, Phys. Rev. Lett. **87**, 040401, (2001).
- [21] M. Li, S.-M. Fei, Z.-X. Wang, J. Phys. A **42**, 145303 (2009).
- [22] M. Siomau and S. Fritzsche, arXiv:1002.3064.